# Global and small-scale structure of the zodiacal dust cloud observed with *AKARI*

Takafumi Ootsubo[1]

[1] *Institute of Space and Astronautical Science, Japan Aerospace Exploration Agency, 3-1-1 Yoshinodai, Chuo, Sagamihara, Kanagawa 252-5210, Japan*

## ABSTRACT

The Solar System is filled with interplanetary dust and its thermal emission dominates the diffuse radiation in the mid- to far-infrared wavelength region. After the advent of infrared astronomical satellites, it was found that there are numerous small-scale structures in the zodiacal emission distribution, including dust-band pairs, a circumsolar ring, and cometary trails, in addition to a smooth background distribution. The dust-band pairs are well studied thus far and are now considered to be associated with disruptive events of asteroid families in the main asteroid belt, which would have occurred within the last 10 Myrs. *AKARI* detects the circumsolar ring and zodiacal dust-band structures at 9, 18, 65 and 90 $\mu$m bands. Furthermore, in the *AKARI* far-infrared map, partial young dust-band candidates can be seen, which are corresponding to the possible bands suggested by the *IRAS* observation. These small-scale structures are important to investigate the recent (<1 Myr) evolution of the dust in the Solar System. Here I summarize the current understanding of the zodiacal emission distribution. I will present the results of the *AKARI* mid- and far-infrared all-sky maps and spectroscopic observations for the global and small-scale structures of the zodiacal dust cloud, and discuss the evolution of the zodiacal dust cloud.

**Keywords:** zodiacal emission, interplanetary dust, comets, asteroids

## 1. INTRODUCTION

In the interplanetary space of our Solar System, small dust grains (typically from $\mu$m to mm) are widely distributed, which are called interplanetary dust (IPD). Zodiacal emission (ZE) is thermal re-radiation of absorbed sunlight by the IPD, and it dominates the diffuse radiation in the mid- to far-infrared (IR) wavelength regime. Since the dust located at around 1 au (astronomical unit) from the Sun has a thermal equilibrium temperature of ~280 K, the ZE dominates the mid-IR brightness of the diffuse emission in the sky. Even in the far-IR regime, the ZE contributes to the sky brightness at high Galactic latitudes, where Galactic radiation is relatively weak.

It is difficult to observe the zodiacal emission precisely from the ground, although the ZE is the strong foreground emission. To determine the brightness distribution of the ZE and the spatial structure of the IPD, full-sky surveys obtained with IR satellites are particularly powerful. The first IR all-sky survey was realized by the *Infrared Astronomical Satellite (IRAS)* in 1983 (Neugebauer et al. 1984a). Subsequent to *IRAS*, the Diffuse Infrared Background Experiment (DIRBE) aboard the *Cosmic Background Explorer (COBE)* satellite conducted an all-sky survey with wider wavelength coverage than *IRAS* (Boggess et al. 1992). The Japanese satellite *AKARI*, a satellite dedicated to IR astronomical observations, was the third mission to survey the whole sky at mid- and far-IR wavelength regions (Murakami et al. 2007).

From the early results of the *IRAS* mission, it was found that the ZE has a smooth global spatial profile. There are, however, also many small-scale structures on a scales of a few to a few tens of degrees (Hauser et al. 1984; Low et al. 1984; Neugebauer et al. 1984b), such as those tracing the asteroidal dust bands and a circumsolar resonance ring (Low et al. 1984; Dermott et al. 1984). In the finer scale of several tens of arcminutes, cometary dust trails of the short period comets are first observed by the *IRAS*. Eaton et al. (1984) found an extremely narrow line of light near the orbit of comet 10P/Tempel for the first time and this structure was called as the cometary dust trail (Sykes et al. 1986). After that, seven more trails around orbits of periodic comets were detected in the *IRAS* survey (Sykes & Walker 1992). These are very fine structures, but it is likely that plenty of relatively large (a few hundred $\mu$m to cm or so) dust grains, as well as small grains, are supplied by comets into the interplanetary space.

*IRAS* also discovered the dust band structures originate from the asteroidal collisions that form small-scale latitudinal features in the ZE. (Low et al. 1984; Neugebauer et al. 1984b). These asteroidal dust bands are seen as the band pair, and there are three major band pairs among the dust bands with respect to the invariant plane of the planets, $i_p = \pm 1\overset{\circ}{.}4, \pm 2\overset{\circ}{.}1$,

Corresponding author: Takafumi Ootsubo
ootsubo@ir.isas.jaxa.jp

and ±9.°3 (Sykes 1988, 1990; Grogan et al. 2001). *COBE*/DIRBE detected the band-pair structures for these asteroidal dust bands (Spiesman et al. 1995; Reach et al. 1997), and observations of ground-based telescopes also confirmed these three structures (Ishiguro et al. 1999a,b). The relationship between observed asteroid families and the *IRAS* dust bands has been a matter of much debate. Dermott et al. (1984) proposed that the dust bands consist of material produced by ongoing collisional grinding of bodies within prominent asteroid families ('equilibrium model'). On the other hand, Sykes & Greenberg (1986) suggested that the *IRAS* dust bands were produced by stochastic breakups of ∼10 km diameter asteroids that occurred in the main-belt region within the last several million years ('nonequilibrium model'). Recent works of detailed dynamical analysis and numerical simulations support the nonequilibrium model. The dust grains released from the asteroid families, which even have small relative velocities of 10–100 m/sec, results in being rapidly distributed into a ring over the parent asteroid's orbit with $10^2$–$10^3$ years. The Jupiter influences on the orbit of the dust ring over a long timescale, and the secular precession of ascending nodes occurs. For the orbit around 2 au, the band pairs extend completely around the ecliptic in about million years. If we observe this structure from the Earth, dense dust at the maximum and minimum latitudes look like a band pair (Sykes & Greenberg 1986). By the numerical modeling, it is suggested that recent breakups ($\lesssim 10^7$ years) of young families/clusters such as Beagle, Karin, and Veritas are the origins of these asteroidal dust bands (Nesvorný et al. 2003, 2008). The dust bands are by-products of recent asteroid breakup events that occur throughout the main belt.

In addition to the asteroidal dust bands and cometary dust trails, there is a structure near the Earth's orbit (the circumsolar ring). The dust falls to the inner region of the Solar System by the Poynting-Robertson (P-R) drag (Burns et al. 1979) in mean motion resonances (MMRs) with the Earth (Jackson & Zook 1989, 1992). It is expected that there are much more dust particles just behind than in front of the Earth. It is noticed that the sky brightness observed by the *IRAS* is higher towards the trailing direction to the Earth's motion than towards the leading direction. *IRAS* and DIRBE detected the blob structure of resonance particles (Dermott et al. 1994; Reach et al. 1995). Spitzer space telescope has a co-moving orbit with Earth and is gradually moving away from the Earth. From the Spitzer observation toward the north ecliptic pole, it is found that trailing blob is a cloud that is centered 0.2 au behind Earth with a width of 0.08 au along the Earth's orbit (Reach 2010).

Small dust in the interplanetary space will fall into or be blown away from the Solar System by the P-R drag, solar radiation pressure by the Sun, and so on. The present distribution of the IPD does not always maintain the initial distribution when the dust was supplied into the interplanetary space. Thus, continuous supply source is needed to maintain the current distribution of dust. It is currently believed that the most of the IPD in the smooth cloud comes from the comets. Near earth regions, in particular, it is estimated that more than 90% dust comes from Jupiter-family comets, and $\lesssim$10% comes from Oort-cloud comets and/or asteroids (Nesvorný et al. 2010).

Thanks to the observations by the past IR space telescopes, such as the spectroscopy with *Infrared Space Observatory (ISO)* and the *Japanese Infrared Telescope in Space (IRTS)* in addition to *IRAS* and *COBE*/DIRBE, the global and small-scale distributions of the ZE is becoming clearer (e.g., Ábrahám et al. 1997; Ootsubo et al. 1998; Leinert et al. 2002; Reach et al. 2003) However, the past IR satellites had limitations, for example, on the mission lifetimes and wavelength coverages. IR satellites with wide wavelength coverage, high spatial resolution, and longer mission lifetime than one year, can reveal the precise global structure and detailed small and fine scale structures of the ZE.

## 2. *AKARI* OBSERVATIONS OF ZODIACAL EMISSION

We performed a full-sky survey with *AKARI*. *AKARI* was an all-sky survey satellite in the mid- and far-IR wavelength regime (Murakami et al. 2007) that was equipped with a cryogenically cooled telescope of 68.5 cm aperture diameter and two scientific instruments, the Far-Infrared Surveyor (FIS: Kawada et al. 2007) and the Infrared Camera (IRC: Onaka et al. 2007). *AKARI* was launched on 2006 February and the all-sky survey was performed during the period of 2006 April to 2007 August, which was the cold operation phase of the satellite. *AKARI* revolved around the Earth in a Sun-synchronous polar orbit and scanned the sky along the circle of the solar elongation at approximately 90° in the all-sky survey. Its 16-month cryogenic mission lifetime is thus far the longest among the far-IR survey missions.

*AKARI*/FIS covers wavelengths longer than 100 $\mu$m and has a higher spatial resolution (1′–1.′5) than *IRAS*. The all-sky far-IR map data[1] have been publicly released (Doi et al. 2015; Takita et al. 2015). Contributions from small-scale ZE structures remain present in the publicly released *AKARI* images, although the smooth component of the ZE is subtracted based on the DIRBE model. Ootsubo et al. (2016) constructed template maps of the asteroidal dust bands and the circumsolar-ring components based on the *AKARI* far-IR all-sky maps[2] (Figure 1). By subtracting the derived dust-band templates, ZE-subtracted *AKARI* far-IR maps well-calibrated in the full-sky region can be obtained (Ootsubo et al. 2016). It is important to obtain a precise estimate of the ZE contribution to the far-IR sky and provide a ZE template and ZE-subtracted far-IR maps based on the *AKARI* data.

The mid-IR all-sky survey was conducted with the two photometric broadband filters centered at 9 $\mu$m (*S9W*) and 18 $\mu$m (*L18W*) of the MIR-S and MIR-L channels, respectively (Onaka et al. 2007; Ishihara et al. 2010). The *AKARI* mid-IR all-sky map data is supposed to be released in public soon (Ishihara et al., in preparation).

[1] The data can be retrieved from http://www.ir.isas.jaxa.jp/ASTRO-F/Observation/

[2] Please contact ootsubo@ir.isas.jaxa.jp or iris_help@ir.isas.jaxa.jp for the dust-band template.

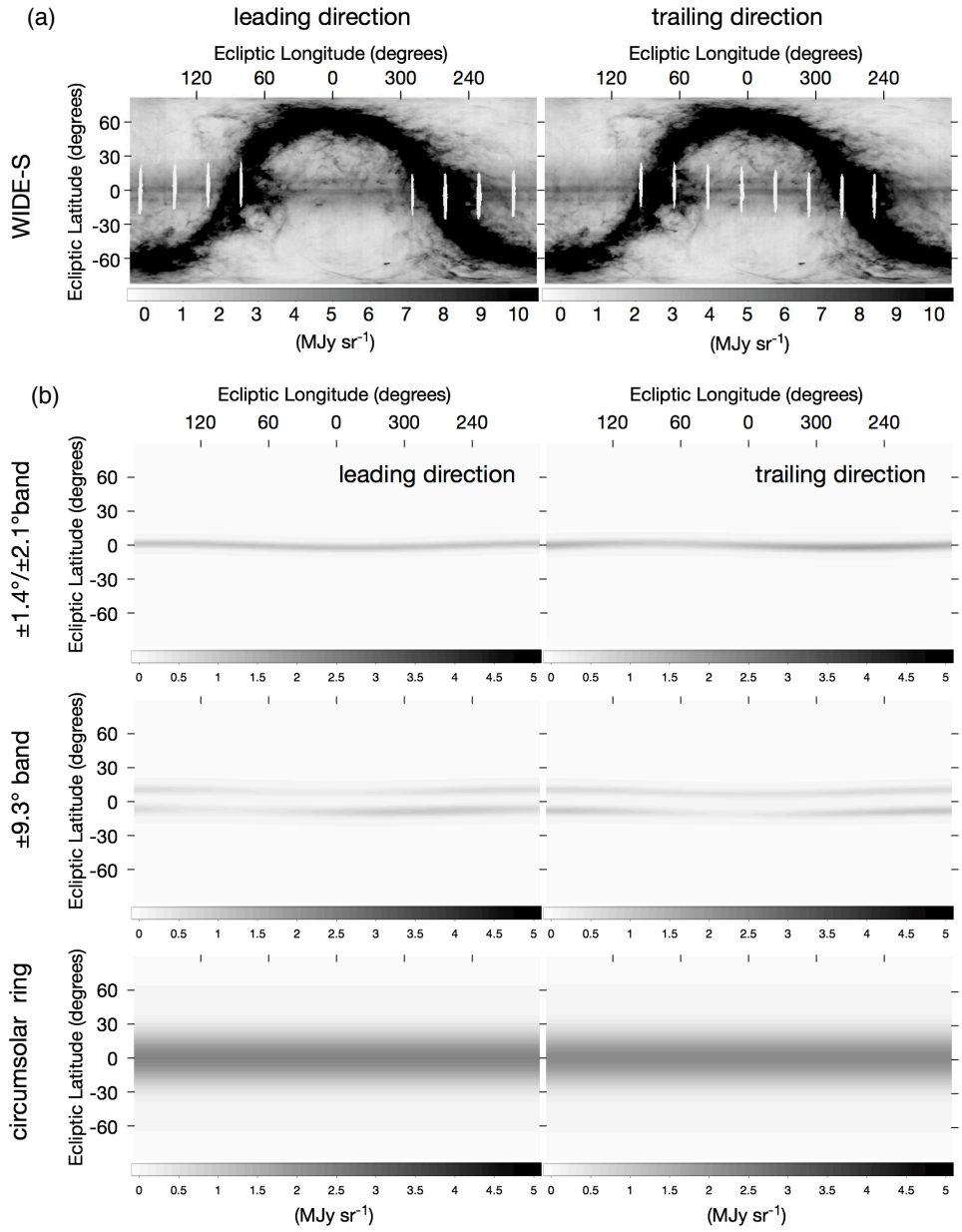


**Figure 1.** (a) *AKARI* far-IR all-sky surface brightness maps in *WIDE-S* (90 $\mu$m) band for the Earth-leading (left-hand panels) and trailing (right-hand panels) directions. The map centers correspond to the sky position (0°, 0°) in ecliptic coordinates. Eight vertically long regions near the ecliptic plane contaminated by Moon light are left blank in each map. (b) Model maps of the dust-band components (decomposed into the $\pm 1.^{\circ}4/2.^{\circ}1$ band, the $\pm 9.^{\circ}3$ band, and the circumsolar ring) in the *AKARI* far-IR maps in the Earth-leading (left-hand panels) and trailing (right-hand panels) directions. Figures are depicted in the same coordinate as the Figure (a).

## 3. GLOBAL AND SMALL-SCALE STRUCTURE OF IPD CLOUD

Many zodiacal dust cloud models have been developed using IR satellite data thus far, including the *IRAS* and *COBE*/DIRBE surveys. Kelsall et al. (1998) made a three-dimensional (3-D) IPD cloud model based on the DIRBE data (hereafter the Kelsall model). To reproduce the sky brightness profile, they divided the IPD cloud complex into the following three components: the smooth cloud, the asteroidal dust bands, and the MMR component (ring and Earth-trailing blob). Wright (1998) also made a ZE model based on the DIRBE data in the similar but the different procedure. Rowan-Robinson & May (2013) estimate the relative contributions of interstellar dust, as well as asteroidal and cometary dust, to the infrared emission from zodiacal dust detected by *IRAS* and *COBE*. They suggest that the interstellar dust is a significant contributor to the local zodiacal dust cloud. The DIRBE ZE model is currently the most popular one to estimate the foreground infrared sky brightness (Kelsall et al. 1998; Wright 1998). However, there is a limitation with the DIRBE model, and obvious residual components of the ZE in the DIRBE mid-IR maps, in particular, for the asteroidal dust bands near the ecliptic plane. This mainly arises from the model fitting procedures that they used limited sky pixels, e.g., every 5° for ecliptic latitudes lower than 30° and every 10° above that for the Kelsall model (Kelsall et al. 1998).

Moreover, earthbound astronomical satellites in the Sun-synchronous polar orbit, including *IRAS*, *COBE*, and *AKARI*, have the limited visibility toward the near-ecliptic region. Accurate modeling of the 3-D IPD cloud has not been successful to reproduce the all-sky spatial distribution of the ZE in the broad IR wavelength region. It is very important to establish the precise ZE model for not only the Solar System science, but also it tremendously has an impact on a wide astronomical science field. Thus, we analyzed the ZE structures in detail with *AKARI* data.

### 3.1. **Smooth cloud**

*AKARI*/IRC conducted the mid-IR all-sky survey with the two photometric broadband filters centered at 9 $\mu$m and 18 $\mu$m (Ishihara et al. 2010). Pyo et al. (2010) compared the preliminary 9 $\mu$m all-sky map with the Kelsall model and found that modifications for the model parameters are needed to reproduce the IRC 9 $\mu$m brightness. Kondo et al. (2016) have carried out the further modeling of the ZE, using the *AKARI* mid-IR all-sky data. They succeeded in improving the modeling of the ZE, and also confirm that their new model better reproduces the ZE in the DIRBE data than the Kelsall model, except for the Earth-trailing blob component (Kondo et al. 2016). They suggest that the vertical offset of the Earth-trailing blob increases by about 0.014 au in the north direction from the *COBE* epoch to the *AKARI* epoch. This may suggest that the dust was recently supplied by comets near the Earth and asymmetrically trapped on the trailing side of the Earth (i.e., a larger amount or closer to the Earth in the north than in the south). Ishihara et al. (2017) report a likely detection of a local interplanetary dust cloud passing near the Earth in the *AKARI* mid-IR all-sky map. The power-law index of the radial distribution for the dust density of the smooth cloud become significantly larger than those of the Kelsall model (from 1.34 to 1.59). The result strongly supports the necessity of such dust supply around 1 au. The results suggest that the size of the smooth cloud, a dominant component in the model, is about 10% more compact than previously thought (Kondo et al. 2016). As for the smooth cloud, it is difficult to obtain the further precise global structure from the data taken by the earthbound satellites. Deep space IR satellites, which observe the ZE at different heliocentric distances (e.g., from the Mars to the Jupiter) in the future, ought to provide the data to capture the whole structure of the IPD smooth cloud.

### 3.2. **Asteroidsl dust bands**

In the mid-IR maps, the dominant contribution of the emission comes from the dust near the Earth. For the far-IR maps, it is not easy to estimate the smooth cloud structure because of its faintness in the far-IR, but it is adequate to study the asteroidal dust bands. Dust particles in the asteroidal dust bands come from the asteroid main belt and distribute around 2 or 3 au from the sun, and the dust grains have the lower temperature than near-earth regions. In the far-IR, however, we need some techniques to measure the dust-band structure precisely, since the galactic dust emission is strong.

Ootsubo et al. (2016) have investigated the geometry of the zodiacal dust bands in the *AKARI* far-IR maps, and constructed template far-IR maps of the asteroidal dust bands and the circumsolar-ring components (Figure 1). From the geometry of the zodiacal dust bands, we can obtain the distance, inclination, and the ascending node of the dust bands (cf. Figure 2). These values are important to make the 3-D IPD distribution model based on the *AKARI* data.

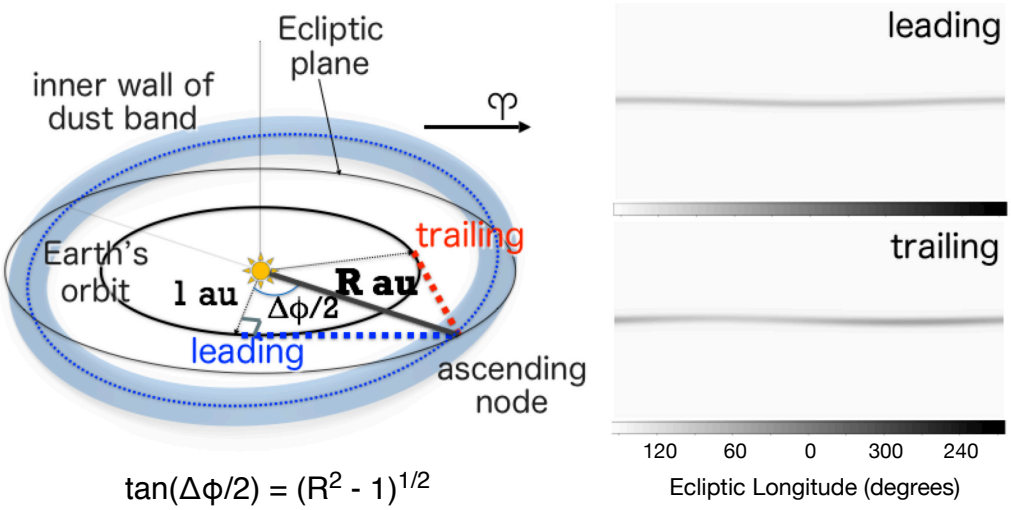


**Figure 2.** A schematic view of the *AKARI* observation of the dust band. *AKARI* observe the ascending node of the dust band at the different positions in the Earth's orbit for the leading and trailing directions. The phase difference between the annual variation of the average latitude of the band pair for scans leading and trailing the Earth can be used to measure the heliocentric distance of the bands.

One of the ways to derive the distance to the dust bands is a parallax estimation. Lines of sight with larger solar elongation intersect the bands closer to the Earth, so that the bands have a greater geocentric angular separation. The variation of band-pair separation with solar elongation depends on the distance to the dust bands. Thus, the distance of the dust bands from the Sun can be determined parallactically from the variation of the band-pair separation as a function of the solar elongation angle (Reach 1992). With the parallax estimation, Reach (1992) found the heliocentric distances of 1.32 ± 0.05 au and 2.04 ± 0.04 au using *IRAS* data for the ±1.4/2.1 and the ±9.°3 bands, respectively. Since near-ecliptic two bands are apparently almost blended and look to be a single band, it is not easy to derive the distance to the ±1.°4 and ±2.°1 bands separately. Hereafter, we refer to this pair as the ±1.°4/2.°1 band. Based on the DIRBE data, Spiesman et al. (1995) derived the parallactic distances of 1.37 ± 0.17 au and 2.05 ± 0.13 au for the ±1.4/2.1 and the ±9.°3 bands, while Reach et al. (1997) found 1.7 ± 0.2 au and 2.4 ± 0.3 au, respectively. Since most *AKARI* scans were limited to a constant solar elongation, $\epsilon \sim 90°$, it is difficult to determine the parallactic distance based on the *AKARI* data. Instead, the phase difference, $\phi$, between the annual variation of the average latitude of the band pair for scans leading and trailing the Earth can be used to measure the heliocentric distance of the bands (Reach 1991). For the dust band structure in the *AKARI* maps, an apparent sinusoidal variation in the ecliptic latitude of the peak position of the dust bands because of a parallax can be seen. From this annual variation of the band latitudes with geocentric ecliptic longitude, and the relation of $\Delta\phi = 2\ \tan^{-1}\sqrt{R^2-1}$, we can get the distance to the inner wall of the asteroidal dust bands, $R$.

Ootsubo et al. (2016) derived the heliocentric distances of the band pairs based on the *AKARI* far-IR 90 $\mu$m maps: 1.86 and 2.16 au for the ±1.4/2.1 and the ±10° bands, respectively. Nesvorný et al. (2006) made simulations of orbital evolution for the dust particles released from the Karin and Veritas family. They found that large particles (~500 $\mu$m) interact with strong secular resonances at a heliocentric distance of ≃2 au, while rapidly drifting small particles experience just modest perturbations. Since *AKARI* results are mainly based on the 90 $\mu$m and 140 $\mu$m band data, large dust particles at further heliocentric distances (>2 au) significantly contribute to the *AKARI* results.

The three major dust-band pairs at ±1.°4, ±2.°1 and ±9.°3 are well studied and are now considered to be associated with known asteroid families (Beagle, Karin, and Veritas), respectively. It is thought that disruption events in the main asteroid belt, which would have occurred within the last $10^7$ years, are major supply sources of dust particles. If the disruption event occurred very recently, for example within $10^6$ years or so from now, then we may detect the partial young dust bands, in the 180° opposite side between northern and southern bands. For example, in the *IRAS* map, potential partial ±6°, ±8° and ±13° band pairs have been suggested in previous studies (Sykes 1988; Reach et al. 1997; Ishiguro et al. 1999a).

Thus, we tried to investigate the partial young dust bands near the ecliptic plane in the *AKARI* far-IR map. Using the image enhanced technique of boxcar-average smoothing subtraction, we extract the structure of width between 1–5° in the latitude direction(cf. Spiesman et al. 1995; Ootsubo et al. 2016).

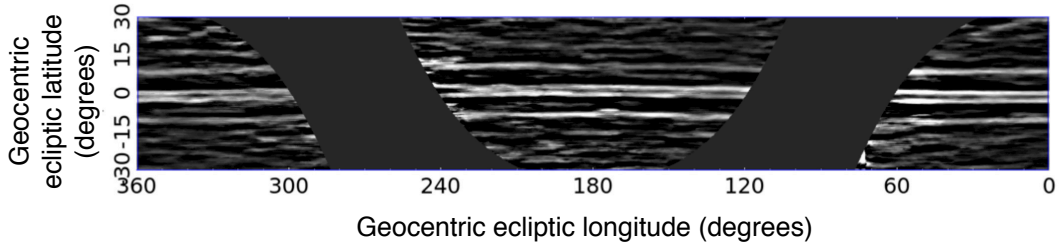


**Figure 3.** The ecliptic plane at 90 $\mu$m as seen by *AKARI*/FIS at the ecliptic latitudes $|\beta| < 30°$. The image is filtered to extract the structures of width between 1–5° in ecliptic latitudes to enhance the dust bands. The Galactic plane region is masked.

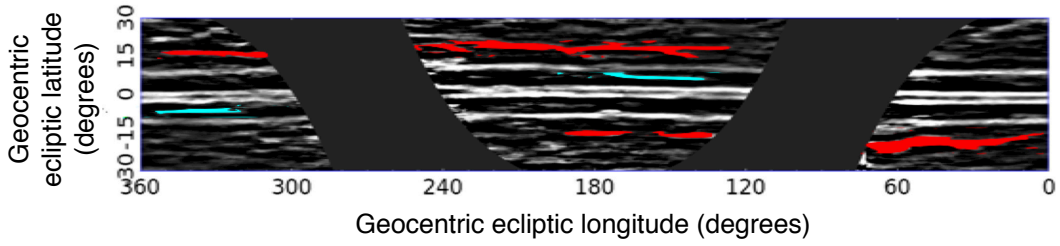


**Figure 4.** The same figure as Figure 3. The ±6° (or ±8°) and 17° band candidates are shown in blue and red, respectively.

We compare the resultant *AKARI* far-IR map with *IRAS* candidate partial dust bands (see figures in Sykes 1990). We can see the dust bands in the *AKARI* map at the similar sky position to the *IRAS* map. Thus far, we detect 2 partial dust-band candidates at the ecliptic latitude of ±6° (or ±8°) and 17°. Recently, it is suggested that 6° band dust is probably released

from Datura cluster, while 17° band originates from Emilkowalski cluster (Espy et al. 2009; Espy Kehoe et al. 2015). It is estimated that these two clusters have the age of less than $10^6$ years. Takaba et al. (in this proceedings) are investigating the dust band structures in the *AKARI* mid-IR all-sky maps. We will confirm these dust-band candidates and extract other fine bands, using the *AKARI* far-IR 65 $\mu$m map and IRC maps together with the 90 $\mu$m map. We can derive the recent dust supply rate in the inner Solar System from the asteroids, if we estimate the surface brightness of the partial young dust bands.

### 3.3. **Cometary trails and circumsolar ring**

We have not yet investigated the cometary dust trails in the *AKARI* maps. After making the all-sky maps with high spatial resolution, we will search the trails. As for the circumsolar ring structure, the peak positions of the circumsolar-ring component are naturally almost all located near the ecliptic plane in the *AKARI* all-sky maps. They do not show any clear sinusoidal change, because *AKARI* observed the dust in the circumsolar ring near the Earth's orbit. In the *AKARI* all-sky maps, we can see the trailing–leading asymmetry of 3.7% in 9 $\mu$m, 3.0% in 18 $\mu$m, and less than 3% in 90 $\mu$m (Ueda et al. 2017; Ootsubo et al. 2016). Ueda et al. (2017) investigated the orbital motion of asteroidal and cometary dust particles considering the gravity of the Sun and the Earth and solar radiation to reproduce the trailing–leading asymmetry. They estimated that asteroidal dust with radius $s \lesssim 3$ $\mu$m and $s \gtrsim 1000$ $\mu$m and cometary dust with $s \lesssim 7$ $\mu$m and $s \gtrsim 300$ $\mu$m show leading–trailing brightness asymmetries comparable to that found by *AKARI* observations.

In addition to the survey data, *AKARI*/IRC had the capability of the pointed spectroscopic observations in the mid-IR regime. Takahashi et al. (in this proceedings) analyzed 74 pointing data obtained in November 2006–August 2007, which has a spectral resolution of $R \sim 50$ in 5–12 $\mu$m. IRC spectra show an excess emission feature in 9–11 $\mu$m which can be reasonably accounted for by a combination of amorphous and crystalline silicate. They also suggest the variations in dust temperature and shape of the feature among different ecliptic latitudes. It is expected that we can derive a difference of the dust mineralogy between observations near the ecliptic plane (especially in the direction of the asteroidal dust bands) and toward the high ecliptic latitude regions.

## 4. **SUMMARY**

Zodiacal emission (ZE) from the interplanetary dust (IPD) dominates the diffuse radiation in the mid- to far-infrared (IR) wavelength regime. It was found that the spatial distribution of the IPD has a smooth global spatial profile, but there are also many small-scale structures, including the cometary dust trails, the asteroidal dust bands, and the circumsolar ring. We investigate the whole picture of the zodiacal dust cloud with *AKARI* mid- and far-IR all-sky maps, which cover almost all the sky with the survey longer than 1 year. We have a plan to construct the 3-dimensional IPD distribution model based on the *AKARI* data, and extract many young asteroidal dust bunds and cometary trails, and derive the detailed property and the supply mechanism of the IPD.

## ACKNOWLEDGMENTS

This research is based on observations with *AKARI*, a JAXA project with the participation of ESA. This work has been supported by JSPS KAKENHI Grant Number 19204020, 25247016, 25400220, and 17K05381. We thank all members of the *AKARI* project, in particular, MP-SOSOS team and *AKARI* FIS/IRC all-sky map team, for their continuous help and support.

## REFERENCES

Abraham, P., Leinert, C., & Lemke, D. 1997, A&A, 328, 702
Boggess, N. W., Mather, J. C., Weiss, R., et al. 1992, ApJ, 397, 420
Burns, J. A., Lamy, P. L., & Soter, S. 1979, Icarus, 40, 1
Dermott, S. F., Jayaraman, S., Xu, Y. L., Gustafson, B. Å. S., & Liou, J. C. 1994, Nature, 369, 719
Dermott, S. F., Nicholson, P. D., Burns, J. A., & Houck, J. R. 1984, Nature, 312, 505
Doi, Y., Takita, S., Ootsubo, T., et al. 2015, PASJ, 67, 50
Eaton, N., Davies, J. K., & Green, S. F. 1984, MNRAS, 211, 15P
Espy, A. J., Dermott, S. F., Kehoe, T. J. J., & Jayaraman, S. 2009, Planet. Space Sci., 57, 235
Espy Kehoe, A. J., Kehoe, T. J. J., Colwell, J. E., & Dermott, S. F. 2015, ApJ, 811, 66
Grogan, K., Dermott, S. F., & Durda, D. D. 2001, Icarus, 152, 251
Hauser, M. G., Gillett, F. C., Low, F. J., et al. 1984, ApJL, 278, L15
Ishiguro, M., Nakamura, R., Fujii, Y., et al. 1999a, ApJ, 511, 432
Ishiguro, M., Nakamura, R., Fujii, Y., et al. 1999b, PASJ, 51, 363
Ishihara, D., Kondo, T., Kaneda, H., et al. 2017, A&A, 603, A82
Ishihara, D., Onaka, T., Kataza, H., et al. 2010, A&A, 514, A1
Jackson, A. A., & Zook, H. A. 1989, Nature, 337, 629
Jackson, A. A., & Zook, H. A. 1992, Icarus, 97, 70

Kawada, M., Baba, H., Barthel, P. D., et al. 2007, PASJ, 59, S389
Kelsall, T., Weiland, J. L., Franz, B. A., et al. 1998, ApJ, 508, 44
Kondo, T., Ishihara, D., Kaneda, H., et al. 2016, AJ, 151, 71
Leinert, C., Ábrahám, P., Acosta-Pulido, J., Lemke, D., & Siebenmorgen, R. 2002, A&A, 393, 1073
Low, F. J., Young, E., Beintema, D. A., et al. 1984, ApJL, 278, L19
Murakami, H., Baba, H., Barthel, P., et al. 2007, PASJ, 59, S369
Nesvorný, D., Bottke, W. F., Levison, H. F., & Dones, L. 2003, ApJ, 591, 486
Nesvorný, D., Bottke, W. F., Vokrouhlický, D., et al. 2008, ApJL, 679, L143
Nesvorný, D., Jenniskens, P., Levison, H. F., et al. 2010, ApJ, 713, 816
Nesvorný, D., Vokrouhlický, D., Bottke, W. F., & Sykes, M. 2006, Icarus, 181, 107
Neugebauer, G., Habing, H. J., van Duinen, R., et al. 1984a, ApJL, 278, L1
Neugebauer, G., Soifer, B. T., Beichman, C. A., et al. 1984b, Science, 224, 14
Onaka, T., Matsuhara, H., Wada, T., et al. 2007, PASJ, 59, S401
Ootsubo, T., Doi, Y., Takita, S., et al. 2016, PASJ, 68, 35
Ootsubo, T., Onaka, T., Yamamura, I., et al. 1998, Earth, Planets, and Space, 50, 507
Pyo, J., Ueno, M., Kwon, S. M., et al. 2010, A&A, 523, A53
Reach, W. T. 1991, ApJ, 369, 529
Reach, W. T. 1992, ApJ, 392, 289
Reach, W. T. 2010, Icarus, 209, 848
Reach, W. T., Franz, B. A., Weiland, J. L., et al. 1995, Nature, 374, 521
Reach, W. T., Franz, B. A., & Weiland, J. L. 1997, Icarus, 127, 461
Reach, W. T., Morris, P., Boulanger, F., & Okumura, K. 2003, Icarus, 164, 384
Rowan-Robinson, M., & May, B. 2013, MNRAS, 429, 2894
Spiesman, W. J., Hauser, M. G., Kelsall, T., et al. 1995, ApJ, 442, 662
Sykes, M. V. 1988, ApJL, 334, L55
Sykes, M. V. 1990, Icarus, 85, 267
Sykes, M. V., & Greenberg, R. 1986, Icarus, 65, 51
Sykes, M. V., Lebofsky, L. A., Hunten, D. M., & Low, F. 1986, Science, 232, 1115
Sykes, M. V., & Walker, R. G. 1992, Icarus, 95, 180
Takita, S., Doi, Y., Ootsubo, T., et al. 2015, PASJ, 67, 51
Ueda, T., Kobayashi, H., Takeuchi, T., et al. 2017, AJ, 153, 232
Wright, E. L. 1998, ApJ, 496, 1